Journal of Biomechanics 45 (2012) 1103–1107

Contents lists available at SciVerse ScienceDirect

Journal of Biomechanics

journal homepage: www.elsevier.com/locate/jbiomech
www.JBiomech.com

Short communication

Calculating the axes of rotation for the subtalar and talocrural joints using 3D bone reconstructions

W.C.H. Parr[a,b,c,*], H.J. Chatterjee[b], C. Soligo[d]

[a] School of Biological, Earth and Environmental Sciences, University of New South Wales, Sydney, NSW 2052, Australia
[b] Research Department of Genetics, Evolution and Environment, Division of Biosciences, University College London, Gower Street, London WC1E 6BT, UK
[c] Department of Palaeontology, Natural History Museum, London SW7 5BD, UK
[d] Department of Anthropology, University College London, 14 Taviton Street, London WC1H 0BW, UK

ARTICLE INFO

Article history:
Accepted 10 January 2012

Keywords:
Ankle joint axis
Subtalar joint axis
3D modelling
Principal axes

ABSTRACT

Orientation of the subtalar joint axis dictates inversion and eversion movements of the foot and has been the focus of evolutionary and clinical studies for a number of years. Previous studies have measured the subtalar joint axis against the axis of the whole foot, the talocrural joint axis and, recently, the principal axes of the talus. The present study introduces a new method for estimating average joint axes from 3D reconstructions of bones and applies the method to the talus to calculate the subtalar and talocrural joint axes. The study also assesses the validity of the principal axes as a reference coordinate system against which to measure the subtalar joint axis. In order to define the angle of the subtalar joint axis relative to that of another axis in the talus, we suggest measuring the subtalar joint axis against the talocrural joint axis. We present corresponding 3D vector angles calculated from a modern human skeletal sample. This method is applicable to virtual 3D models acquired through surface-scanning of disarticulated 'dry' osteological samples, as well as to 3D models created from CT or MRI scans.

© 2012 Elsevier Ltd. All rights reserved.

1. Introduction

The average axis of rotation of the talus over the calcaneus at the subtalar joint (STJ) has long been the focus of evolutionary studies (Elftman and Manter, 1935; Gebo, 1992, 1993; Lewis, 1980, 1989; Morton, 1922, 1924, 1927) and clinical studies (Beimers et al., 2008; Manter, 1941). This is because it has undergone realignment in modern humans, compared to the STJ axes in non-human primates and is not well defined clinically (Beimers et al., 2008; Fournol, 1999). In their recent paper on subtalar joint (STJ) axes orientation, Beimers et al. (2008) used the principal axes (PA) as the reference coordinate system against which to measure the STJ axis angles. The PA are calculated by performing a singlular value decomposition of the 3D coordinates of each virtual talus so that the 1st principal axis (*x*-axis) defines the long axis of the talus. The manipulation and CT-scanning of feet in different positions as performed by Beimers et al. (2008) is likely to give very good results for establishing STJ axis angles within individuals, but has the disadvantage of exposing patients to repeated doses of radiation and of being unsuited for patients with reduced foot mobility. It also cannot be applied to osteological samples as commonly used in inter-specific comparative studies.

1.1. Aims

To provide a non-invasive approach for estimating joint axes for individual specimens or patients that is applicable to 3D models generated from CT, MRI or surface laser scan data. Specifically, the present study:

- Introduces a new method for estimating the compromise STJ and talocrural joint (TCJ) axes from the surface morphology of virtual 3D models of human tali.
- Assesses the existing method of using the PA of each individual talus as reference axes to measure the STJ axes against.
- Defines a reliable 3D method for quantifying the relationship between STJ and TCJ axes.

2. Materials and methods

58 disarticulated modern human tali (Supplementary Table 1) from the collections of the Palaeontology Department at the Natural History Museum (NHM), London, were digitised through surface laser scanning using a Konica Minolta Vivid 910 surface laser scanner. The scanner is accurate to *X*: ±0.22 mm, *Y*: ±0.16 mm, *Z*: ±0.10 mm. Virtual model point density needs to be sufficient to allow for the articular facets to be accurately identified. Surface scanning and

* Corresponding author at: Rm 558, School of Biological, Earth and Environmental Sciences, Biological Sciences building (D26), University of New South Wales(UNSW), Sydney, NSW 2052, Australia. Tel.: +61 405658783.
E-mail addresses: parr.will@googlemail.com (P. W.C.H.), h.chatterjee@ucl.ac.uk (C. H.J.), c.soligo@ucl.ac.uk (S. C.).

0021-9290/$ - see front matter © 2012 Elsevier Ltd. All rights reserved.
doi:10.1016/j.jbiomech.2012.01.011

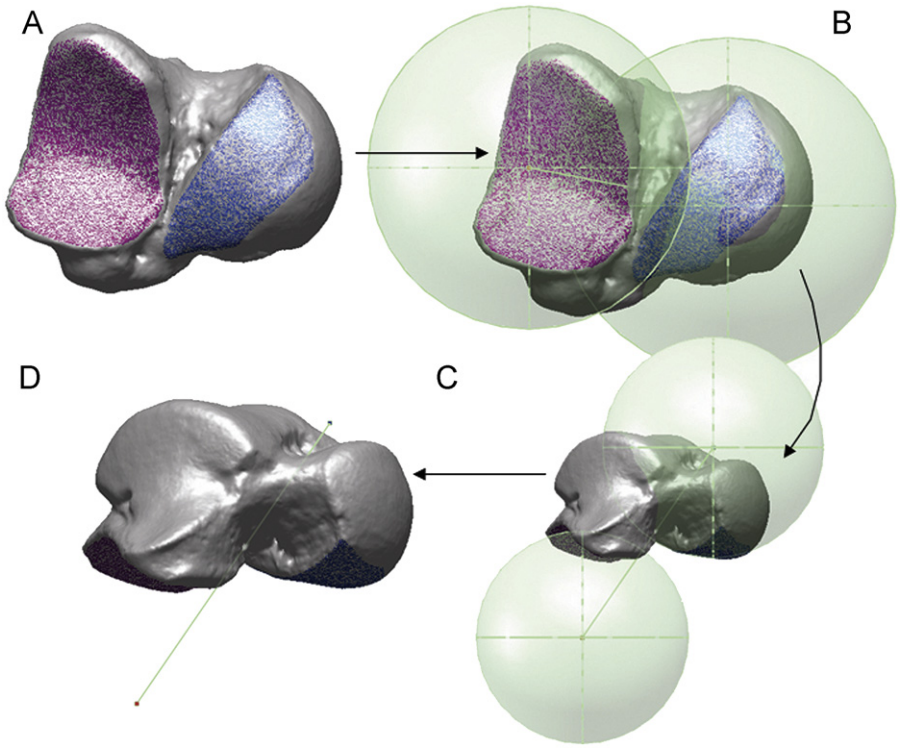

Fig. 1. Flow diagram showing the method for calculating the subtalar joint axis on a right talus. A) Plantar view showing the calcaneal facet highlighted in purple (left hand facet) and the sustentaculum facet highlighted in blue (right hand facet). B) Same as A), with spheres fitted to calcaneal and sustentaculum facet surfaces. C) Lateral view of B) showing the two centre points of the spheres and the vector joining them. D) Lateral view of the talus with calculated subtalar joint axis. (For interpretation of the references to color in this figure legend, the reader is referred to the web version of this article).

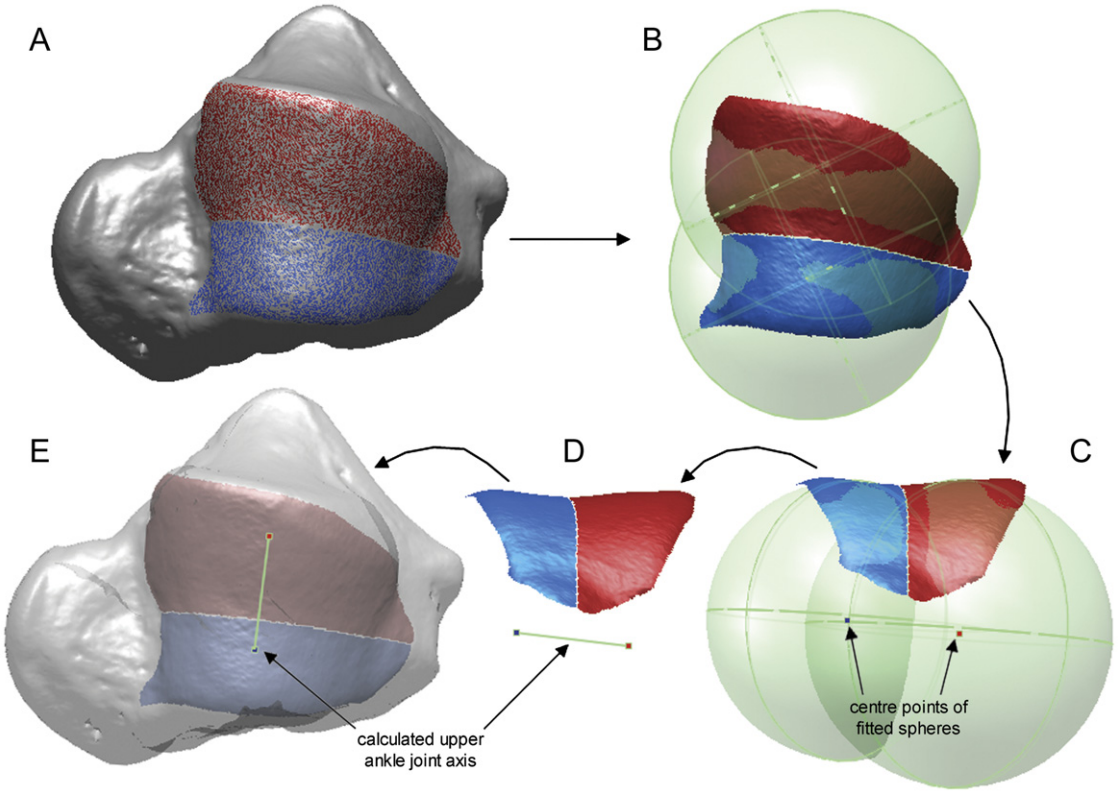

Fig. 2. Fig. 2. Flow diagram showing the method for calculating the talocrural joint axis on a right talus. A) Dorsal view showing the medial half of the trochlea highlighted in blue (lower half of facet) and lateral half highlighted in red (upper half of facet). B) Dorsal view of the trochlea with spheres fitted to its medial and lateral halves. C) Posterior view of B) showing the two centre points of the spheres. D) and E) The talocrural joint axis is calculated as the vector joining the centre points of the spheres. (For interpretation of the references to color in this figure legend, the reader is referred to the web version of this article).

model construction follow established procedures (Parr et al., 2011a, b). Each virtual talus was centred with its centroid at the origin of the 3D Cartesian coordinate system. The tali were then registered with one another using an Iterative Closest Point (ICP) algorithm (Besl and Mckay, 1992), which minimises differences in tali orientation using whole surface morphology. Angular differences between the orientations of the PA of individual tali within the global coordinate space were then calculated.

The talar STJ axis is determined by the morphology of the sustentaculum (anterior, or mid- and anterior, plantar) and the calcaneo (posterior plantar) facets. Spheres were fitted to the surfaces of these facets using least squares minimisation. The centre points of these spheres represent good approximations of the centre points of rotation around each of the facets (Fig. 1). The average STJ axis was estimated as the 3D vector passing through these points. Once the STJ vector is determined, 2D angles between combinations of axes in 3D space can be calculated: "deviation" and "inclination" in Beimers et al. (2008). For comparison with the results of Beimers et al. (2008), their angles for eversion-dorsiflexion to inversion-plantarflexion movements were used, as these are expected to give the fullest range of motion at the STJ.

For estimating the TCJ axis from the trochlea surface morphology, we found that sphere fitting to the medial and lateral half of the trochlea facet was the most reproducible method as each half can be defined as the facet surface between the central trochlea groove and the medial or lateral rim (Fig. 2). The 3D vector between the two sphere centre points is the TCJ axis estimate. To create two intersecting vectors, the STJ and TCJ vectors were translated so that one end of each vector was at the origin of the coordinate system. The resulting 3D vector angles are used as the quantitative measure of the relative orientation of the two ankle joint axis to each other.

Traditionally studies have reported the orientation of the STJ with respect to the midline of the anatomical position of the foot (Inman, 1976; Isman and Inman, 1969). The present study considers the shape of the talus alone and so information regarding the orientation of the talus within the foot is lost.

3. Results

There are clear similarities between the STJ axes calculated here (Fig. 3A) and those calculated from the in-vitro studies of Beimers et al. (2008) (Fig. 3B), Manter (1941) (Supplementary Fig. 1) and

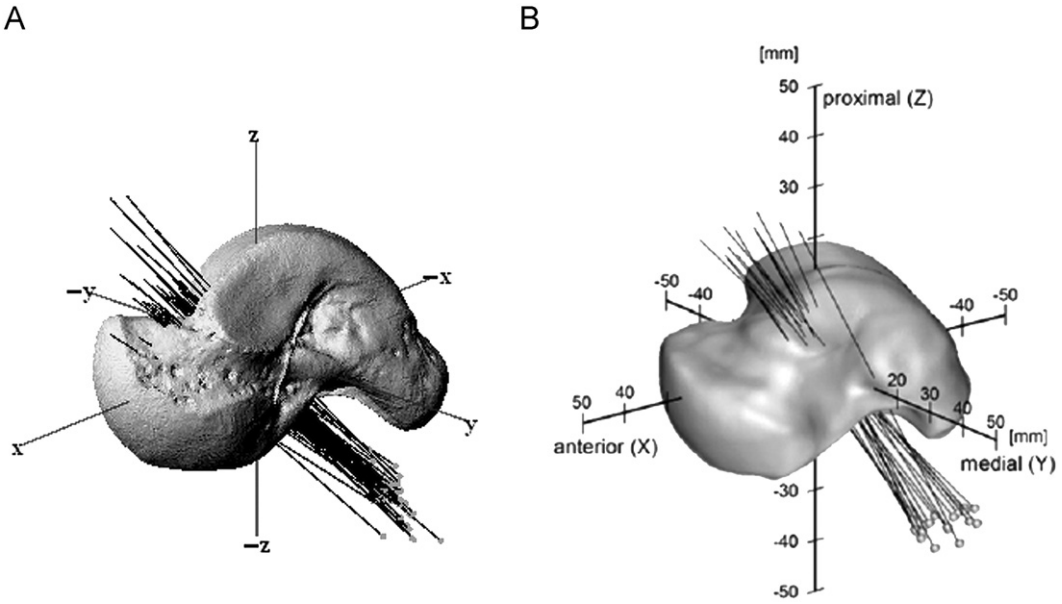

Fig. 3. A) Talus shown with its principal axes and with the calculated STJ axes for our sample using the method introduced in the present study. B) Figure adapted from Beimers et al. (2008) showing a talus with its principal axes and all 20 of the experimentally obtained subtalar joint axes (for eversion-dorsiflexion to inversion-plantarflexion movements alone) for their sample.

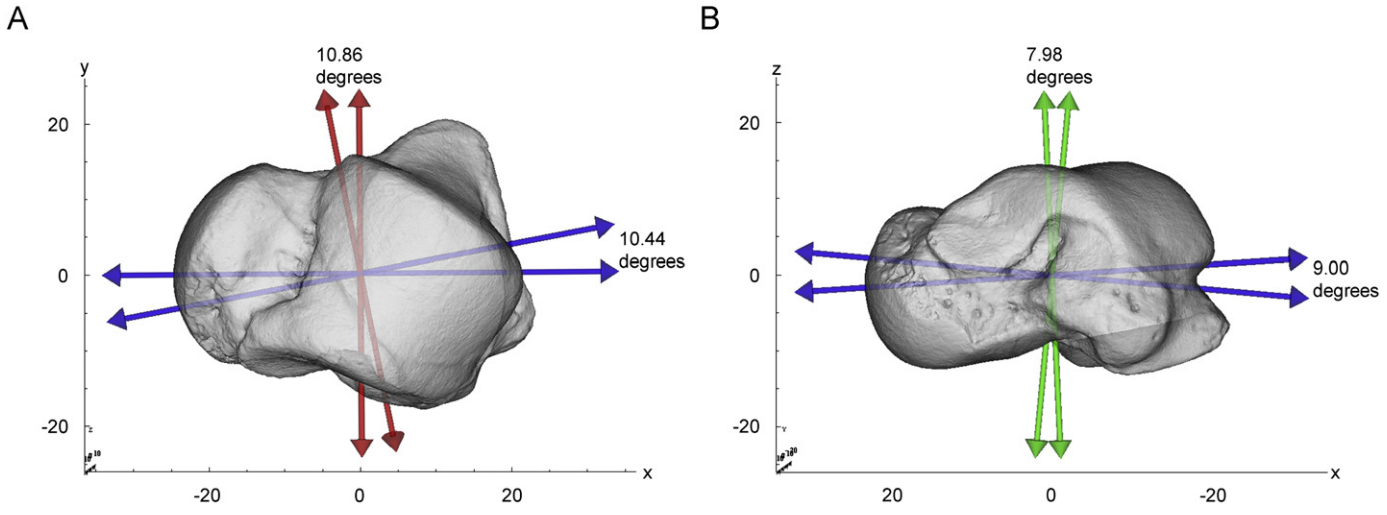

Fig. 4. Variation in the calculated principal axes for the tali used in this study. A) Shows variation in the sagittal plane view for the *x* (blue, horizontal axes in A) and *y* (red, vertical axes in A) principal axes. B) Shows variation in the transverse plane view for the *x* (blue, horizontal axes in B) and *z* (green, vertical axes in B) principal axes. The *x* and *z* principal axes in the sagittal and transverse planes were used by Beimers et al. (2008) to calculate the angles of deviation and inclination, respectively, for the STJ axis. Note the variation in the calculated *x* (blue), *y* (red) and *z* (green) principal axes. (For interpretation of the references to color in this figure legend, the reader is referred to the web version of this article).

Nester (1998) (Supplementary Fig. 2), suggesting that the method for defining the STJ axis introduced in the present study is accurate.

There was considerable range in the PA calculated for each individual talus. The range between maximum and minimum deviation values of the first principal axis in the *XY* plane (blue axes in Fig. 4A) is 10.4°, in the *XZ* plane (inclination) the range is 9.0° (blue axes in Fig. 4B). The range in deviation of the second principal axis in the *XY* plane is 10.9° (red axes in Fig. 4A). The range in inclination of the third principal axis in the *XZ* plane is 8.0° (green axes in Fig. 4B).

When measured against the PA for each specimen the STJ axes calculated in the present study are partially consistent with those calculated by Beimers et al. (2008). The present study calculated a mean angle of deviation (2D angle in the *XY* plane) of 5.0° (SD=3.4°; Table 1) and a mean angle of inclination (2D angle in the *XZ* plane) of 45.5° (SD=3.8°; Table 1). Beimers et al. (2008) calculated a mean angle of deviation of 11.8°, with a standard deviation of 8.0°, which includes our mean estimate. However, for the angle of inclination Beimers et al. (2008) calculated a mean of 50.9°, with a standard deviation of 4.0°, which does not include our mean estimate.

Table 1
Angles of deviation and inclination of the STJ axis as calculated against the principal axes of each talus specimen (as in Beimers et al., 2008).

	Angle of deviation	Angle of inclination
Mean	5.0	45.5
Median	4.5	45.5
Standard deviation	3.4	3.8
Maximum	12.9	53.0
Minimum	−2.6	38.6
Range	15.5	14.4

Table 2
3D vector angles calculated between STJ and talocrural joint axes.

	3D vector angle in degrees
Mean	62.3
Median	61.9
Standard deviation	3.5
Maximum	70.6
Minimum	54.7
Range	15.9

Our method of defining the talocrural and STJ axes and calculating the angle in 3D space between these two axes gave a mean angle of 62.3°, with the standard deviation of 3.5° and range of 15.9° (Table 2, Fig. 5, Supplementary Figs. 3 and 4). Testing for differences in mean 3D vector angles between populations and sex revealed no statistically significant differences in either case (Populations: Kruskal–Wallis test, $df=5$, $\chi^2=7.316$, $p=0.20$; Sex: *t*-test, $df=50$, $t=1.075$, $p=0.29$).

4. Discussion

The range in the first principal axis measured in the *XZ* plane (9.0°) represents a substantial proportion of the variation seen in the corresponding angle of inclination reported by Beimers et al. (2008) (14.0°). The range of the first principal axis in the *XY* plane is 10.4°, which may have contributed to the large variation (27.4°) in the angle of deviation reported by Beimers et al. (2008). These differences in PA orientation that we have demonstrated are likely caused by the globular nature of the talus, which lacks bilateral symmetry, and indicate that the use of the PA as the reference coordinate system for quantifying the orientation of the STJ axis introduces an element of error.

The projections of angles between 3D vectors onto coordinate system planes are not independent of each other, a fact that is routinely overlooked in the literature. The separate reporting of maximum deviation and inclination angles is of limited biological relevance, since the individual with the maximum angle of deviation is unlikely to also be the one with the maximum inclination. Other descriptive statistics derived from those values (mean, range, standard deviation) similarly lack biological relevance. They are presented here to provide an accurate comparison between our results and the results of earlier studies.

The need to treat joint axes and their relationships with each other as a multivariate problem is illustrated in Supplementary Figs. 3 and 4, where the range of individually projected values frequently exceed the maximum and minimum values based on the combined STJ and TCJ axes angles. A fully biologically relevant quantification of STJ and TCJ axis orientations requires an approach of the type introduced here in the form of the vector angle in 3D space calculated between the two axes, or where unit vector coordinates are entered into a multivariate analysis (Greiner and Ball, 2009), which is beyond the scope of this technical note.

As the vector angle in 3D space is calculated between two joint axes, the angle contains more functional information than the angles of inclination and deviation. The mean 3D joint axes angle

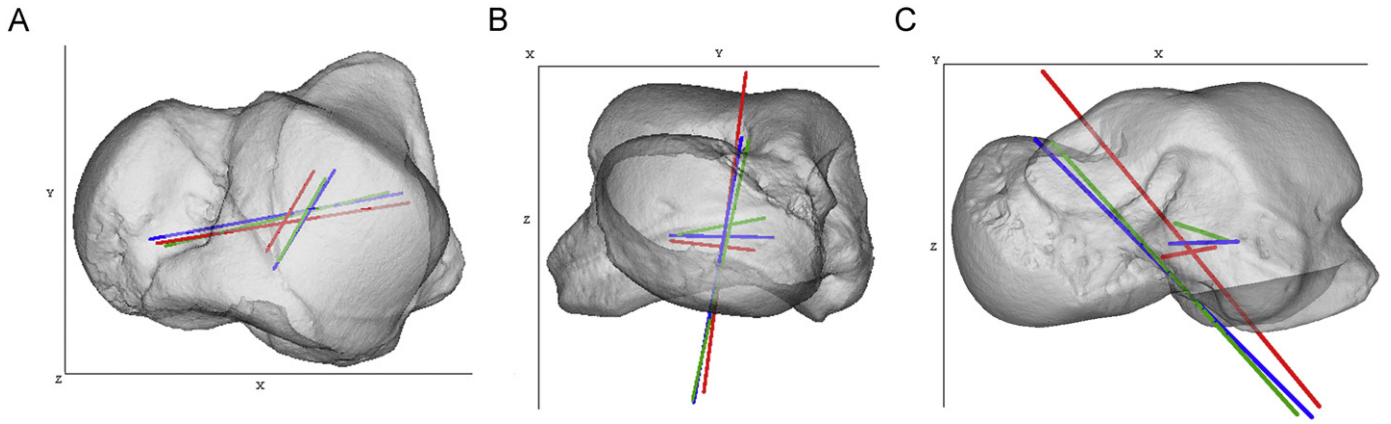

Fig. 5. Talus specimen showing talocrural and STJ axes corresponding to the mean (blue), maximum (red) and minimum (green) angles between talocrural and STJ axes. A) Sagittal plane view, B) frontal plane view (C) transverse plane view. Talus specimen is at 55% opacity to show the path of the axes. Planes and axes are in accordance with Wu et al. (2002).

is at around 60°. If this were a typical "universal joint" this angle would be 90°, which suggests a level of synchronization in these two joint axes. Within our human sample, the metric looks to be relatively conserved, as we detected no significant differences between either populations or sex in our samples.

Conflict of interest statement

The authors have no conflicts of interest to report.

Acknowledgements

We thank Norman Macleod for access to the NHM's Konica Minolta scanner and the following curators and their institutions for access to material: Charles Lockwood, Department of Anthropology, UCL; Robert Kruszynski and Margaret Clegg, Department of Palaeontology, NHM, London. Financial support to William Parr came from NERC (Award no: NER/S/A/2004/12187) with additional funding through a CASE award from the NHM, London, and recently an Endeavour Award Postdoctoral Research Fellowship (Award no: 2359-2011).

Appendix A. Supporting materials

Supplementary data associated with this article can be found in the online version at doi:10.1016/j.jbiomech.2012.01.011.

References

Beimers, L., Tuijthof, G.J.M., Blankevoort, L., Jonges, R., Maas, M., Van Dijk, C.N., 2008. In-vivo range of motion of the subtalar joint using computed tomography. Journal of Biomechanics 41, 1390–1397.

Besl, P.J., Mckay, N.D., 1992. A method for registration of 3-D shapes. IEEE Transactions on Pattern Analysis and Machine Intelligence 14, 239–256.

Elftman, H., Manter, J., 1935. The evolution of the human foot, with especial reference to the joints. Journal of Anatomy 70, 56–76.

Fournol, S., 1999. L'arthroplastie totale sous-talienne. Resultats et bilan d'une serie de 100 protheses. Medical Chirurgie Pied 15, 67–71.

Gebo, D.L., 1992. Plantigrady and foot adaptation in African Apes—implications for hominid origins. American Journal of Physical Anthropology 89, 29–58.

Gebo, D.L., 1993. Functional morphology of the foot in primates. in: Gebo, D.L. (Ed.), In Postcranial Adaptations in Nonhuman Primates. University Press. Illinois, Northern Illinois.

Greiner, T.M., Ball, K.A., 2009. Statistical analysis of the three dimensional joint complex. Computer Methods in Biomechanics and Biomedical Engineering 12 (2), 185–195.

Inman, V.T., 1976. The Joints of the Ankle. Williams and Wilkins, Baltimore.

Isman, R.E., Inman, V.T., 1969. Anthropometric studies of the human foot and ankle. Bulletin of Prosthetics Research 10, 97–129.

Lewis, O.J., 1980. The joints of the evolving foot. 2. The Intrinsic Joints. Journal of Anatomy 130, 833–857.

Lewis, O.J., 1989. Functional Morphology of the Evolving Hand and Foot. Clarendon Press, Oxford.

Manter, J.T., 1941. Movements of the subtalar and transverse tarsal joints. The Anatomical Record 80, 397–410.

Morton, D.J., 1922. Evolution of the human foot I. American Journal of Physical Anthropology 5, 305–336.

Morton, D.J., 1924. Evolution of the human foot II. American Journal of Physical Anthropology 8, 1–52.

Morton, D.J., 1927. Human origin. American Journal of Physical Anthropology 10, 173–203.

Nester, C., 1998. Review of literature on the axis of rotation at the sub talar joint. The Foot 8, 111–118.

Parr, W.C.H., Chatterjee, H.J., Soligo, C., 2011a. Inter- and intra-specific scaling of articular surface areas in the hominoid talus. Journal of Anatomy 218, 386–401.

Parr, W.C.H., Ruto, A., Soligo, C., Chatterjee, H.J., 2011b. Allometric shape vector projection: a new method for the identification of allometric shape characters and trajectories applied to the human astragalus (talus). Journal of Theoretical Biology 272, 64–71.

Wu, G., Siegler, S., Allard, P., Kirtley, C., Leardini, A., Rosenbaum, D., Whittle, M., D'Lima, D.D., Cristofolini, L., Witte, H., Schmid, O., Stokes, H., 2002. ISB recommendation on definitions of joint coordinate system of various joints for the reporting of human joint motion—part 1: ankle, hip, and spine. Journal of Biomechanics 35, 543–548.